

Article

“Group Inversion Approach” for Detection of Soil Moisture Temporal-Invariant Locations

Claudia Notarnicola

EURAC-Institute for Applied Remote Sensing, Viale Druso 1, 39100 Bolzano, Italy;

E-Mail: claudia.notarnicola@eurac.edu; Tel.: +39-0471-055-375; Fax: +39-0471-055-389

Received: 26 October 2009; in revised form: 9 December 2009 / Accepted: 14 December 2009 /

Published: 21 December 2009

Abstract: This paper presents an approach denominated *Group Inversion Approach (GIA)* which aims at detecting soil moisture temporal invariants, *i.e.*, the stable temporal soil moisture locations, by using mainly remotely sensed data. The soil moisture temporal invariants are those locations where independently of the absolute value changes, the relative spatial distribution of soil moisture remains almost constant. In this procedure, the soil moisture values estimated from different inversion approaches and sensor configurations are compared among themselves and with the ground data. The procedure has been tested in a watershed of around 7,000 km² with data collected during the SMEX’02 experiment in Iowa (USA). The results indicate that fields with inversion errors lower than five times the soil moisture variability detected with ground measurements represent well the mean watershed soil moisture values. The GIA technique has been also found in good agreement with the classical technique used to detect the stable soil moisture features, based exclusively on ground measurements.

Keywords: soil moisture; radar data; ground measurements; inversion approach; temporal stability

1. Introduction

Soil moisture is a key variable for the understanding of geological, hydrological and climatic phenomena. The knowledge of prior soil moisture in a basin is an important factor for hydrological and erosion modeling [1].

Soil moisture determination by ground measurements is often hampered by its high spatio-temporal variability as a result of atmospheric and local redistribution processes which may depend on soil

texture, roughness and vegetation. For these purposes, remotely sensed data can offer good perspectives for monitoring temporal and spatial soil moisture variations. In particular, SAR (Synthetic Aperture Radar) data have proven useful in the detection of soil moisture since they are very sensitive to its variations, even though some limitations in the retrieval accuracy still persist [2].

These two sources of information, ground truth and satellite estimates, are often compared and used as complementary data. In fact, the validation approach between ground measurements and sensors estimates is quite challenging because the *in-situ* measurements are carried out at a scale which is orders of magnitude smaller than the sensors' footprints, thus introducing biases and errors in the validation. In this context, one important issue is how to relate these two different types of measurements.

Along with the mismatch in scale between satellite footprints and ground measurements, another important factor is the high spatial and temporal variability of soil moisture [3]. Based on this analysis, a large number of ground measurements are required to validate a single sensor measurement, thus determining a network of measurements highly dense in the study area.

Experimental works, mainly based on *in-situ* soil moisture measurements, have indicated that spatial soil moisture patterns can be stable in time and then highly correlated with the mean soil moisture over a bigger area, usually a watershed [4]. This indicates that in these locations, even if the absolute soil moisture value changes, the relative spatial distribution of soil moisture remains almost stable over the whole area. Then having established such a relation between local and areal measurements, the estimates of soil moisture coming from coarse remotely sensed data could be upscaled to determine local soil moisture information.

In this context, Vachaud *et al.* [4] proposed an analysis of soil temporal stability to develop a method in order to reduce the number of measuring points. The basic idea of this technique is that a soil moisture field may maintain its spatial pattern over time and that certain sampling points express the mean behaviour of the whole study area. If a field is found stable, the mean of the field at a given time is then compared to the specific sampling site in order to identify locations with small bias to the mean and a low variability in its relationship to the field mean values. This idea was initially proven in a 2,000-m² grassland field in Grenoble (France).

Greyson and Western [5] extended this research to several other watersheds such as the Tarrawarra catchment (Australia; mostly dryland grazing), Chickasha (OK, USA; mostly pasture and winter wheat), and Lockyersleigh (Australia; a mixture of grazing land and woodland).

Furthermore, Kachanosky and De Jong [6] introduced the idea that spatial scale, such as the correlation length scale has to be considered in this kind of analysis, so that the temporal stability it is also a function of scale. Numerous other authors [7-9] have addressed the problem of spatial and temporal variability of soil moisture content.

How to relate coarse resolution satellite data to finer scale measurements is important, not only for validation purposes, but also because most of the next generation sensors will have only a coarse resolution (25–50 km).

This paper illustrates an approach to detect stable soil moisture locations based on the comparison between the soil moisture estimate errors and the field intrinsic variability as measured on the ground. One main difference with respect to the classical approach presented by Vachaud *et al.* [4] is that this

procedure is not only based on ground measurements, but takes it into account the soil moisture estimates derived from SAR sensors.

The paper is organized as follows. In Section 2, the experimental data set is introduced. Section 3 is devoted to the description of the inversion procedures and how their results are merged in the new method, called *Group Inversion Approach (GIA)*. The preliminary results are illustrated in Section 4 where they are also compared with the results obtained by a traditional technique. Section 5 draws conclusions, envisaged application and future developments of the proposed approach.

2. Experimental Data Sets

The experimental data set is a subset of data acquired during the SMEX'02 Experiment that took place in Iowa (USA) from June 24–July 12, 2002. The study area was chosen in order to obtain microwave and optical observations over a range of soil moisture conditions with moderate to high vegetation biomass conditions. During the experiment, both radar and optical remotely sensed data were acquired.

The main site was the Walnut Creek watershed, where 32 fields, mainly cultivated with soybean and corn, were sampled intensively. The field and sensor data acquired during this experiment are particularly suitable to our analysis because of:

- the number of fields that were considered in the experiment with different level of soil and vegetation moisture;
- the acquisition of both radar and optical data and the extensive ground measurements carried out within each field.

The fields analyzed in this work are five soybean fields WC03, WC09, WC10, WC13 and five corn fields WC01, WC05, WC06, WC08, WC12. Table 1 illustrates the main field characteristics. The AirSAR images (resolution: 8–12 m ground range) were acquired on 1, 5, 7, 8, 9 July 2002. The Landsat (resolution: 30 m) images were acquired 1, 8 July 2002.

The five L- and C-band images were processed by the AirSAR operational processor providing calibrated data sets. The absolute and relative calibration accuracy obtained for each sensor, as reported in the literature [10], are: ± 1.0 dB / ± 0.4 dB for C band, ± 1.2 dB / ± 0.5 dB for L band.

During the campaign, two Landsat Thematic Mapper (TM) scenes from Landsat 5 and three Landsat Enhanced Thematic Mapper plus (ETM+) from Landsat 7 were acquired during the primary study period. The images were atmospherically and radiometrically corrected to produce the at-ground reflectance and then the NDVI and NDWI indices. In this work, the data acquired on 1st July and some data taken randomly from the other dates were considered as training samples. The fact to not consider exclusively the data coming from one single day allows the results to be independent from the specific soil and weather conditions of a single date.

Contemporary to these sensor acquisitions intensive ground measurements were carried out for the determination of the soil and vegetation characteristics. For the most part, soil moisture sampling was performed on sites approximately a quarter section (0.8 km by 0.8 km) in size. 14 points were sampled in a field for a variety of variables, but gravimetric samples were only taken at four sites.

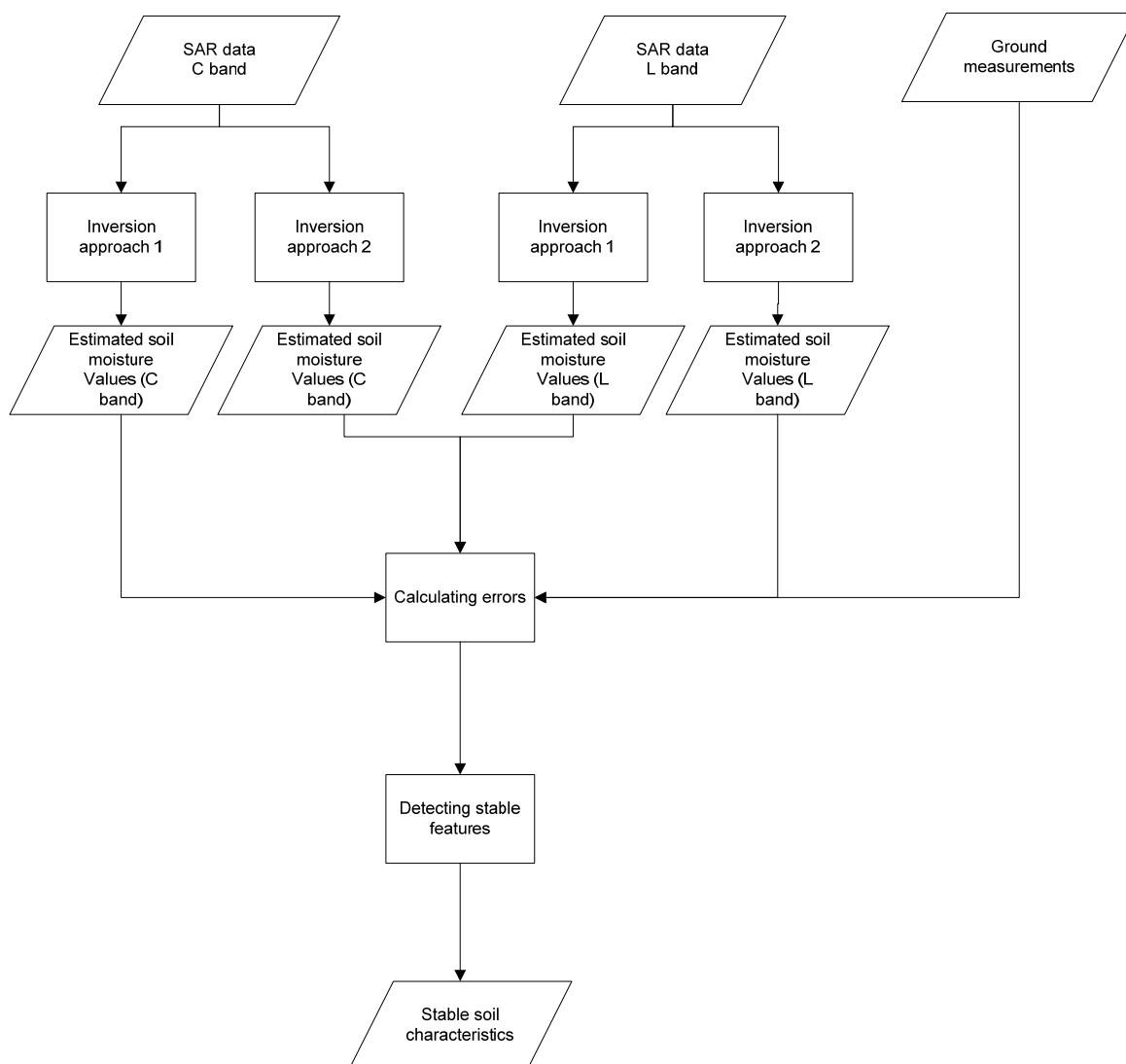
Table 1. Some characteristics of the SMEX'02 fields analyzed in the work.

Fields	Roughness range	Volumetric soil moisture range	Vegetation	Biomass range (kg/m ²)	Vegetation water content (kg/m ²)
WC01	0.67 cm ≤ s ≤ 2.14 cm 1.55 cm ≤ l ≤ 17.68 cm	14% ≤ mv ≤ 27%	Corn	2.17–7.46	3.50–4.70
WC03	0.34 cm ≤ s ≤ 0.72 cm 1.40 cm ≤ l ≤ 13.05 cm	11% ≤ mv ≤ 29%	Soybean	0.13–0.41	0.36–0.88
WC05	0.67 cm ≤ s ≤ 1.83 cm 3.48 cm ≤ l ≤ 5.92 cm	10% ≤ mv ≤ 16%	Corn	1.14–2.36	3.70–4.76
WC06	0.37 cm ≤ s ≤ 0.73 cm 3.06 cm ≤ l ≤ 10.55 cm	9% ≤ mv ≤ 24%	Corn	0.35–2.23	3.88–4.61
WC08	0.85 cm ≤ s ≤ 2.56 cm 2.32 cm ≤ l ≤ 19.19 cm	9% ≤ mv ≤ 24%	Corn	1.06–1.62	3.66–4.78
WC09	0.41 cm ≤ s ≤ 1.10 cm 1.91 cm ≤ l ≤ 14.74 cm	9% ≤ mv ≤ 25%	Soybean	0.28–0.60	0.45–0.92
WC010	0.41 cm ≤ s ≤ 1.10 cm 5.15 cm ≤ l ≤ 16.06 cm	7% ≤ mv ≤ 27%	Soybean	0.21–0.75	0.74–1.28
WC012	0.64 cm ≤ s ≤ 1.65 cm 8.17 cm ≤ l ≤ 16.94 cm	7% ≤ mv ≤ 14%	Soybean	1.06–2.32	3.50–4.60
WC013	0.33 cm ≤ s ≤ 1.35cm 0.47 cm ≤ l ≤ 11.17 cm	10% ≤ mv ≤ 24%	Soybean	0.10–0.42	0.29–0.66

3. The Group Inversion Approach

The developed approach aims at detecting stable features by comparing the estimated soils moisture values from two or more inversion approaches with measured soil moisture values. The basic idea behind this approach is that the stable soil moisture features are found where all the inversion procedures converge to the same estimated values. In many cases, soil moisture instability is often due to some features such as drainage, texture, roughness and local slope. As the inversion algorithms are designed to work on wide areas by taking into account general fields conditions, these specific features may not be properly described in the inversion algorithms thus determining high errors. Consequently, by analyzing different inversion algorithms, it is possible to highlight situations where these factors emerge.

In this study the analysis is limited to two main inversion approaches, already extensively validated and tested on numerous data sets: one based on a Bayesian techniques and the other on an empirical technique. Furthermore, the estimated soil moisture values have been compared among each other in order to understand if the stable soil moisture points can be detected by using only remotely sensed derived data. The overall procedure is illustrated in Figure 1. In the following paragraphs, the two inversion procedures are briefly introduced.

Figure 1. The overall procedure used to detect soil stable characteristics.

3.1. The Bayesian approach

This approach has been developed for bare soils and then extended to vegetated fields as indicated in Notarnicola *et al.* [11,12]. The inversion procedure is mainly based on a Bayesian approach for the calculation of the posterior probability density function derived from the training data. The results of the procedure applied to SMEX'02 indicate that the rmse of the estimated soil moisture data in comparison with ground measurements varies from 6% to 8% for L band and C band, respectively.

3.2. The empirical approach

The Bayesian approach described above has been compared with a classical inversion method. The method follows an empirical approach developed by Chen *et al.* [13] and based on a previous work by Dubois *et al.* [14]. Within the 32 fields, twelve of them have been chosen randomly and considered as training fields by taking into account both soybean and corn fields and different moisture conditions. The training and test data used in this approach are the same used in the Bayesian procedure. On the

backscattering coefficients and soil moisture, a multiple linear regression has been performed where the volumetric soil moisture mv is linearly correlated to the backscattering coefficients for HH and VV polarizations. A further correction Δmv is imposed to this relationship in order to take into account the effect of the different levels of vegetation (soybeans and corn) and the different kinds of interaction of vegetation with a C-band and an L-band signal.

The term Δmv has been added for C-band, because the extracted soil moisture values are constantly underestimated for both soybean and corn fields in dry soil conditions. In fact, the maximum effect of vegetation water content on a C-band signal is for dry soil conditions when the signal from bare soil is very low and can be neglected with respect to the vegetation contribution.

The correction factor has been calculated as a mean value of the difference between extracted and measured soil moisture values for soybean and corn fields of the training set. This mean value is $0.08 \text{ cm}^3/\text{cm}^3$.

For L-band, the extracted soil moisture values are constantly underestimated for soybean fields in all soil moisture conditions. For this signal frequency the low values of vegetation amount of soybean has little impact on radar signal. Then, the correction factor has been calculated as a mean of the differences between extracted and measured soil moisture values for soybean fields of the training set. This mean value is $0.10 \text{ cm}^3/\text{cm}^3$.

The RMSE of the estimated soil moisture data in comparison with ground data varies from 4% to 7% for L band and C band respectively. The rmse obtained in this case is lower than the one obtained for the Bayesian approach. However, while the Bayesian approach is developed in a general contest, this empirical model can be hardly exported to other data sets.

3.3. The Group Inversion Approach: Basic Theory

The Group Inversion Approach (GIA) aims at putting together the results from different inversion approaches with pointy ground measurements. It defines the context and the limit of the comparison between field averages of the estimated soil moisture with an average value derived from point measurements taken on the ground as described in Settle [15].

Considering a squared area A , with side S , three functions can be defined:

- $s_t(x,y)$, that represents the spatial distribution of soil moisture detected by the SAR sensor; in this case the main hypothesis is that the soil moisture patterns are detected by the radar backscatter [16]. To reduce the effect of speckle, the images have been multi-looked;
- $g_t(x,y)$, that represents the spatial distribution of soil moisture detected by the ground measurements;
- $m_t(x,y)$ that is the 'real' spatial distribution of soil moisture within the considered area.

The subscript t indicates that these variables are considered at time t . From function $s_t(x,y)$ through the inversion procedure an average value of soil moisture m_S is determined. From ground measurements, another average m_G is obtained. In this application, the variables introduced are the following:

- $m_{S,t}$: is the average of the SAR-inferred soil moisture values;
- $m_{G,t}$: is the average of the ground point measurements of soil moisture;
- $\text{Var}_t(0)$: is the variance of the ground point measurements of soil moisture.

A function $d_t(x,y)$, is defined which expresses the difference between the sensor function and the ground truth function:

$$[d_t(x,y) = s_t(x,y) - g_t(x,y)] \quad (1).$$

Then the quantity of interest is the difference between the two averages:

$$\Delta m_{S-G,t} = m_{S,t} - m_{G,t} = \int d_t(x,y) m_t(x,y) dx dy \quad (2).$$

Spatial variability of soil physical properties, such as soil moisture, within and among agricultural fields is inherent in nature, due to geological and pedologic forming factors. The variability can also be induced by management practices as well as by the presence of vegetation. These factors interact with each other across spatial and temporal scales.

The spatial distribution $m_t(x,y)$ can be split into terms, one pertinent to a regional trend R and one pertinent to a residual trend δ that are not correlated each other [15]:

$$m_t(x,y) = R_t(x,y) + \delta_t(x,y) \quad (3).$$

Then the difference term can be expressed as follows:

$$\Delta m_{S-G,t} = \Delta m_{R,t} + \Delta m_{\delta,t} = \int d_t(x,y) R_t(x,y) dx dy + \int d_t(x,y) \delta_t(x,y) dx dy \quad (4).$$

For soil moisture, the term R is mainly driven by atmospheric events and has generally a correlation length higher than one kilometre. As this study deals with measurements at field level, it may be assumed to vary slowly within the considered area A and its contribution to the integral (4) can be neglected. In other terms, R is not expected to considerably change over the length of the area that in turn is representative of the sampled fields. This assumption cannot be done for the term δ because it depends on local phenomena and can vary quickly from one pixel to the other.

The term deriving $\Delta m_{\delta,t} = m_{\delta S,t} - m_{\delta G,t} = \int d_t(x,y) \delta_t(x,y) dx dy$ from the residual function δ_t is of interest. As δ_t can be considered a stochastic variable with zero mean, both $m_{\delta S,t}$ and $m_{\delta G,t}$ are also stochastic variables with zero mean. It is expected that over a large number of samples their difference has to be small. However, as both variables are calculated on a finite (sometimes small) number of samples, a bias will exist if one is considered as an estimate of the other. For both variables, their values can change according to the area considered.

The squared difference is expressed as follows:

$$\Delta m_{\delta,t}^2 = \left[\int d_t(x,y) \delta_t(x,y) dx dy \right]^2 = \int d_t(x,y) d_t(u,v) \delta_t(x,y) \delta_t(u,v) dx dy du dv \quad (5)$$

and its expectation value is:

$$E(\Delta m_{\delta,t}^2) = \int d_t(x,y) d_t(u,v) E(\delta_t(x,y) \delta_t(u,v)) dx dy du dv \quad (6).$$

The last value depends on how δ_t is correlated at the points defined (x,y) and (u,v) . Between $r = (x,y)$ and $s = (u,v)$ there could be defined an autocorrelation function with a characteristic length, L :

$$E(\delta_t(r) \delta_t(s)) = \text{Var}_t(0) \rho_t\left(\frac{\|r-s\|}{L}\right) \quad (7).$$

where $\text{Var}(0)$ is the variance of δ_t and ρ_t is the autocorrelation function. If the initial difference $\Delta m_t = m_{S,t} - m_{G,t}$ is considered, the expected squared difference can be written as:

$$E(\Delta m_{S-G,t}^2) = \Delta m_{R,t}^2 + \xi_t^2 \text{Var}_t(0) \quad (8).$$

where $\Delta m_{R,t}^2$ is the square of the error resulting from the regional trend and the term:

$$\xi_t^2 = \int d_t(r) d_t(s) \rho_t \left(\frac{\|r-s\|}{L} \right) dr ds \quad (9)$$

indicates how much the point variability in the surface fluctuations, given by $\text{Var}_t(0)$, is transferred to an error in the area average [15].

The trend term $\Delta m_{R,t}^2$ is neglected, considering that its correlation length is sufficiently large and hence determines little variations of $m_{R,t}$ in the field. Then the term $\xi_t^2 = E(\Delta m_{S-G,t}^2) / \text{Var}_t(0)$ has been calculated as the ratio between the squared difference of the average of the satellite-inferred data and the average of the point measurements and the variance of the point measurements. The numerator of ξ_t^2 is related to the calculation of the RMSE between retrieved soil moisture values and ground measurements. This value is then weighted with the soil moisture spatial distribution, expressed by the denominator. ξ_t^2 characterizes the size of the error obtained by smoothing an underlying field, and then considering the averaged value as a point measurement. In other terms, it is the error associated with taking a point measurement to represent a large area average thus transferring the variability of the surface parameter into an estimate uncertainty.

4. Results

4.1. Results from the Group Inversion Approach

For the 10 fields of the SMEX'02 data sets, the soil moisture values have been estimated by considering the two inversion techniques applied separately to C and L band and for four acquisition dates. The inversion procedures have been applied both considering a mean value of backscattering coefficient for each field and applying the procedure on a pixel-per-pixel basis and then averaging the results. Each of these four retrieved soil moisture values has been compared with ground measurements and the ξ_t^2 values have calculated as indicated previously. As a subsequent step, in order to understand at what level the retrieved soil moisture values are stable, the ground measurements have been skipped and the retrieved values have been compared to each other, considering as a reference the soil estimates of the Bayesian procedure for C and L band. In this analysis the different approaches are the following:

- Bay-mean (C): the Bayesian approach applied to C band data on mean backscattering coefficients for each field,
- Bay-mean (L): the Bayesian approach applied to L band data on mean backscattering coefficients for each field,
- Bay-mean (Cref): the Bayesian approach applied to L band data on mean backscattering coefficients for each field. The estimates are compared with the estimates derived from the inversion approach applied to C band and not to ground measurements,
- Bay-mean (Lref): the Bayesian approach applied to C band data on mean backscattering coefficients for each field. The estimates are compared with the estimates derived from the inversion approach applied to L band and not to ground measurements,

- Emp-mean (C): the empirical approach applied to C band data on mean backscattering coefficients for each field,
- Emp-mean (L): the empirical approach applied to L band data on mean backscattering coefficients for each field,
- Bay-pixel (C): the Bayesian approach applied to C band data on a pixel basis and then averaging the results for each field,
- Bay-pixel (L): the Bayesian approach applied to L band data on a pixel basis and then averaging the results for each field.

The results of comparison among the different algorithms applied to C and L band are illustrated in Figure 2. The highest ξ_t^2 values are found for the empirical procedure applied to C band data and for the comparison of the L band estimates with the C band estimates considered as ground truth. Two important features emerge from this analysis. One is related to the temporal variation. On 5 July there was a heavy rain and then in the following days, it was possible to follow the dry-down phase. In fact the errors increase with time, soon after the rain the soil is more homogeneous while in the dry down phase, different patterns appear related to vegetation, rows and soil textures. The second aspect is related to the temporal stability of some fields. In particular fields WC09 (soybean) and WC01 (corn) present always very low values of ξ_t^2 for all the days and inversion procedures. In this work, the low values of ξ_t^2 are supposed to be associated to field temporal stability.

Figure 2. The error ξ_t^2 variability due to the different algorithms and acquisition dates (5 July, 7 July, 8 July and 9 July).

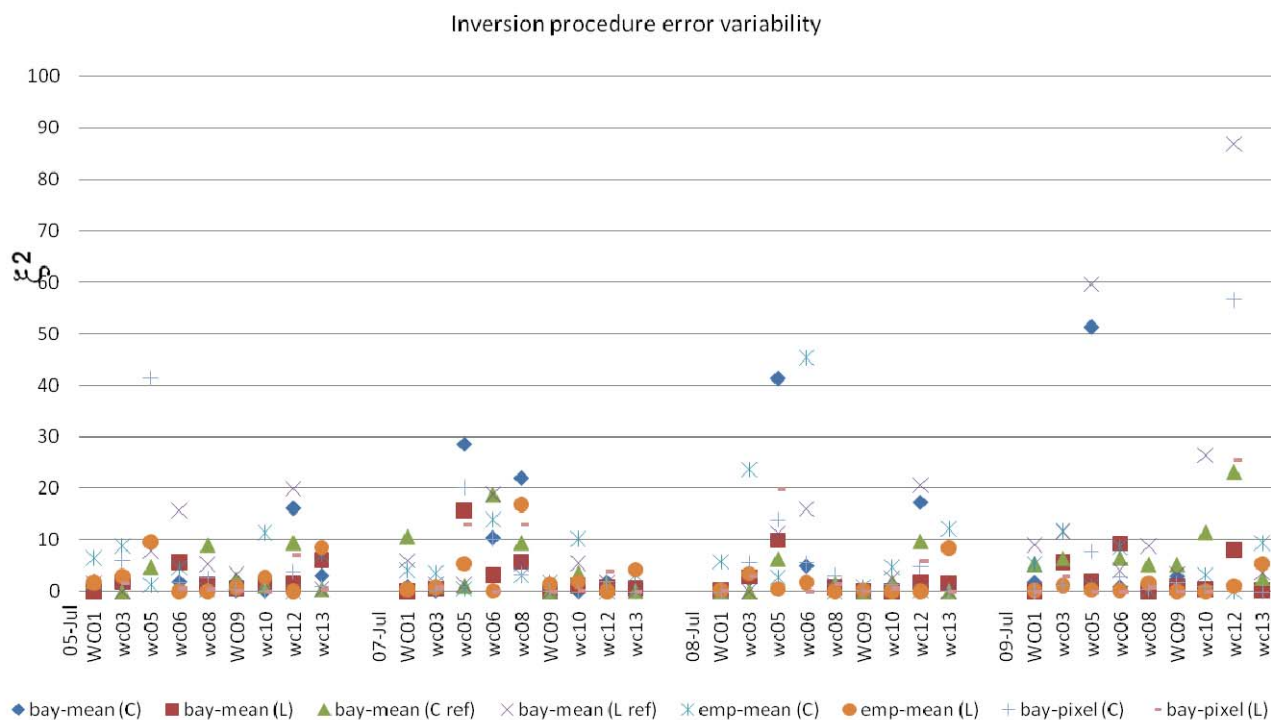


Figure 3 illustrates the mean errors of the inversion procedures with the ± 1 standard deviation, while Figure 4 indicates the mean temporal values for each field. Taking into account these results,

some fields show the lowest errors in all the considered dates and for all the retrieval techniques. For these fields, considered as temporal stable fields, the mean values of soil moisture measured on the ground are compared with the mean value derived from the whole watershed. The results are presented in Figure 5 while Table II reports the regressions statistics of the relationship between mean field soil moisture and mean watershed soil moisture.

Figure 3. The error variability ξ_t^2 for each field and for each analyzed date. The errors have been averaged on all inversion algorithms. The error bars are ± 1.0 standard deviation with respect to the mean value. The graph reports also temporal trend indicating the increased variability after the rain event of 5 July.

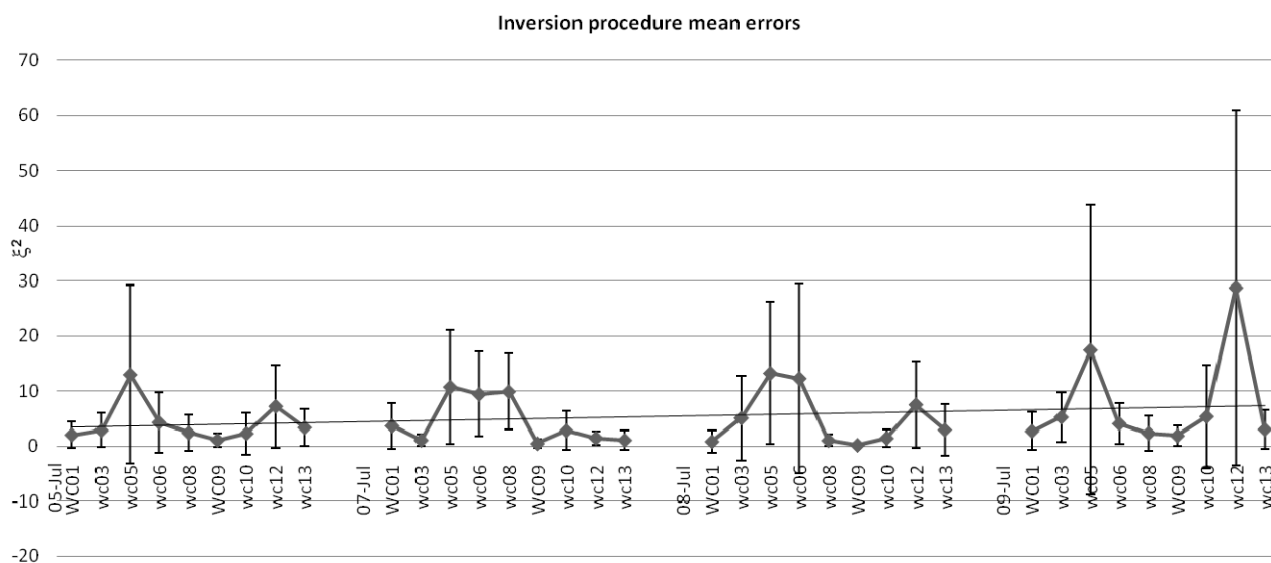


Figure 4. The error ξ^2 variability for each field is reported. The errors have been averaged over all inversion algorithms and all four dates. The error bars are ± 1.0 standard deviation with respect to the mean value.

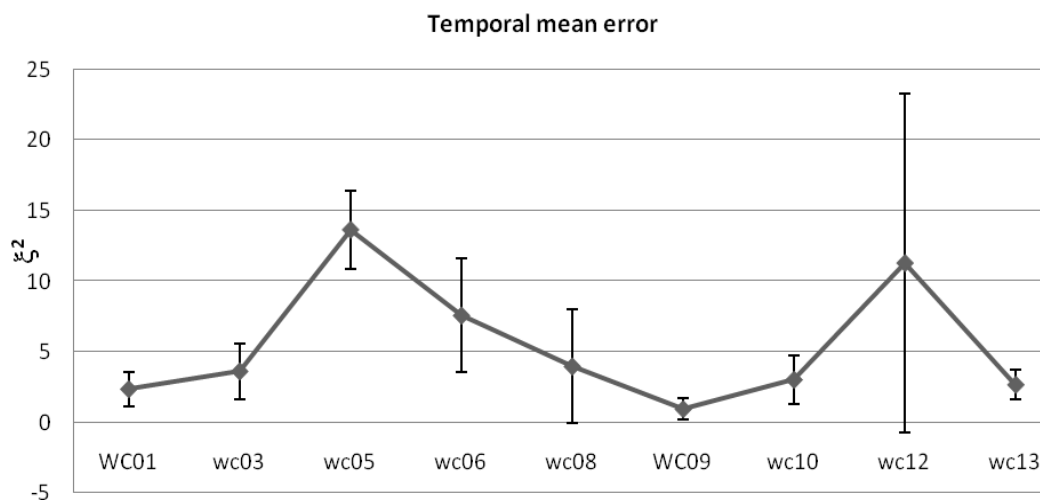
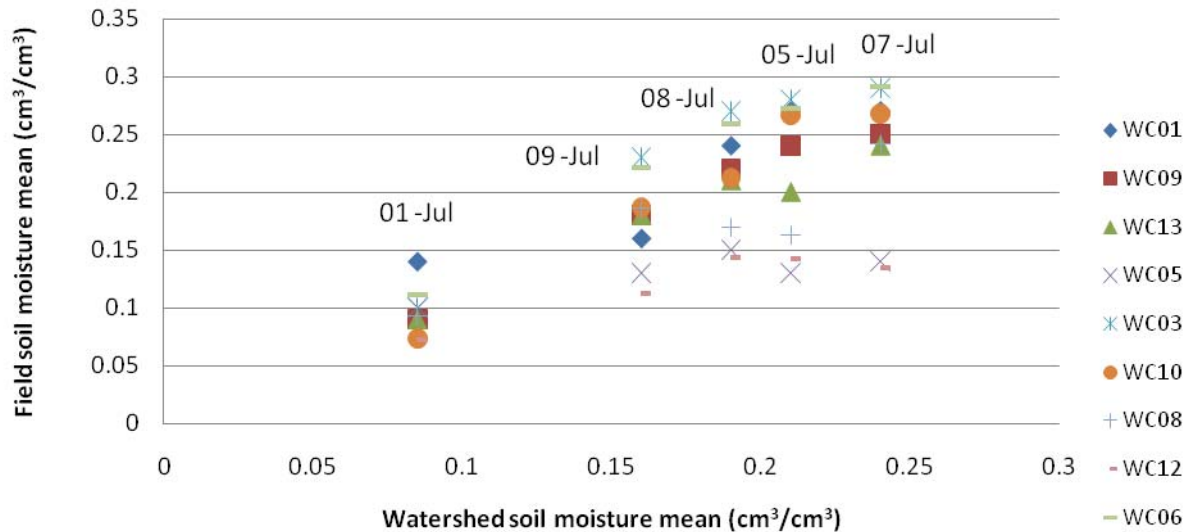


Figure 5. Comparison between the watershed soil moisture mean values and the field soil moisture mean values for fields that were considered as stable (WC 01, 09, 13) and as non stable (WC05, 12).



Fields WC 01, WC 09, WC 13, WC10 present the lowest errors in all inversion procedure and dates. They can be considered as stable fields representative of the watershed mean soil moisture levels. WC 05 and WC12 are fields with the highest errors for all the inversion techniques and show a net deviation from the watershed mean. WC08, WC10 and WC06 also show a good correlation with the watershed mean even though they tend to overestimate (WC08, 10) or under estimate (WC 06) the watershed mean.

Some parameters could be identified as the forcing factors that cause specific time-invariant stability factors. The most common factors are: the precipitation, the soil texture which determines the water-holding capacity, the slope of land which regulates run-off and infiltration and vegetation which determines evapo-transpiration and deep percolation [17]. In this context, the contribution of precipitation plays two different roles. It determines a temporary effect on soil moisture patterns. Soon after the rain event, precipitation water smoothes the difference among different patterns of the same field. This difference becomes to appear as the dry-down phase starts. Furthermore, when the soil is wet due to rain the signal coming from soil is stronger and the impact of vegetation on the retrieved values of soil moisture is less evident. This combined effect is evident from Figure 2, where the inversion errors for the July 5 and 7 are lower than the other two days.

From the correlation between the field and the watershed mean, it emerges fields with ξ_r^2 values lower than 5, that is where the expected squared difference between the estimates and the ground measurements is lower than around five times the field variability $\text{Var}(0)$, can be considered stable and represent the average behavior of the whole watershed.

Fields WC05 and WC 12 exhibit peculiar characteristics among the analyzed fields. WC05 is a dry field with the lowest variability among all fields. Furthermore, this field has the highest local slope, calculated as the ratio between the standard deviation of height and the correlation length, with respect

to all the other analyzed fields. WC 12 is the only field with drainage features. The drainage features determine a horizontal distribution of water thus resulting in non-stationary soil moisture fields [18].

Table 2. Regression statistics of the relationship between mean field soil moisture and mean watershed soil moisture.

	Bias (cm³/cm³)	R²	Slope	RMSE (cm³/cm³)
WC01	0.04	0.84	0.96	0.044
WC05	0.08	0.68	0.26	0.062
WC09	0.004	0.97	1.08	0.021
WC13	0.018	0.95	0.94	0.013
WC03	0.007	0.935	1.281	0.061
WC10	0.032	0.964	1.326	0.033
WC08	0.03	0.772	0.792	0.026
WC12	0.08	0.68	0.261	0.063
WC06	0.02	0.971	1.191	0.056

4.2. Comparison between the GIA and Traditional Methodology Results

The results obtained with the GIA have been also compared with the time stable point assessment introduced by Vachaud *et al.* [4], based on point ground measurements. This technique considers the $\theta_{i,j,t}$ that is the volumetric soil moisture content (VSM) at location i , at field j and time t to calculate the relative mean difference as:

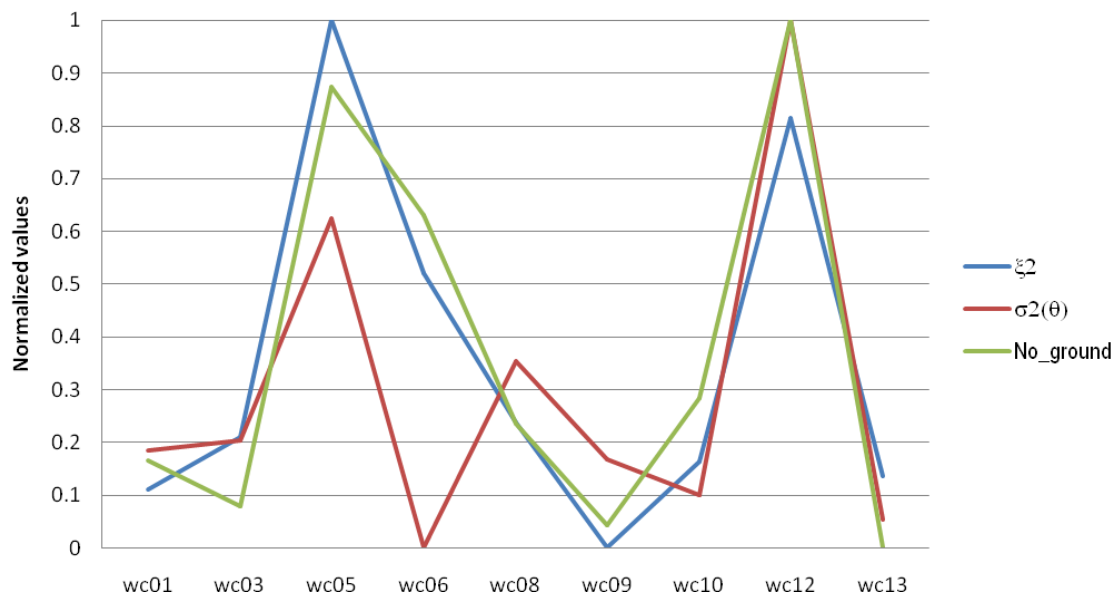
$$\bar{\mu}_j = \frac{1}{n_t} \sum_{t=1}^{n_t} \frac{\theta_{i,j,t} - \overline{\theta_{j,t}}}{\overline{\theta_{j,t}}} \quad (10)$$

where $\overline{\theta_{j,t}}$ is the mean of VSM for each field at time t , n_t is the number of dates. The mean relative difference allows highlighting the difference, in terms of constancy in temporal stability, between sampling locations. Then, the variance of the mean relative difference, $\sigma^2(\mu)$, is calculated as an estimator of temporal stability [19]. For the calculation of $\sigma^2(\mu)$, the volumetric soil moisture values determined at four standard locations in each site were considered. Volumetric soil moisture values are calculated by using gravimetric soil moisture and bulk density that are the parameters directly measured in the fields. The gravimetric soil moisture (GSM) was sampled on each day of sampling with a 0–6 cm scoop tool. GSM is converted to volumetric soil moisture (VSM) by multiplying gravimetric soil moisture and bulk density of the soil. Bulk density was sampled one time at each of these four locations using an extraction technique.

The values of $\sigma^2(\mu)$ and of ξ^2 are then normalized with respect to the respective minimum and maximum values in order to be comparable for ranking. The results shown in Figure 6 indicate a good agreement between the two methodologies. In this graph the case “No_ground” has also been introduced in order to verify the results when the ground measurements are not taken into account in the GIA approach. The Spearman rank analysis has been carried out on these values indicating a significant correlation between the data at the 95% level of confidence if field WC 06 is excluded.

The different behaviour of the methodologies is mainly due to the field vegetation status of field WC06. This field is divided in two parts, one almost completely bare and the other part covered by dense vegetation. On the contrary, the inversion procedure used in this case is particularly calibrated for dense vegetated fields, thus determining a higher error value in soil moisture estimation in the part where the vegetation is not present.

Figure 6. Comparison between the errors calculated with the GIA method present in this paper and the classical methodology introduced by Vachaud *et al.*, [4]. The case “No_ground” indicates when the ground measurements are skipped in the GIA approach.



5. Conclusions and Future Developments

The presented work presents a novel approach for the individuation of stable field characteristics starting from the soil moisture estimates derived from different inversion approaches and sensor configurations. These soil moisture estimates have been compared to ground measurements and among each other. The comparison indicates that there are some particular field characteristics where all the soil moisture estimates converge. The fields which have these characteristics show a good agreement with the watershed soil moisture means. The results of the new approach have been also found in good agreement with results from the traditional approach exclusively based on ground measurements.

The presented approach is particularly useful because:

- the field stable features can be estimated from the SAR images directly;
- the comparison between the soil moisture estimates reveals the same behavior of the comparison between soil moisture estimates and soil moisture ground measurements;
- this analysis can be useful in order to improve and better understand the upscaling and downscaling processing when passing from local to areal soil moisture estimation and *vice versa*;

- In fact, an important application of this analysis is that starting from these stable fields can be inferred information of soil moisture on wider area. On the contrary, starting from images with coarse resolution such as scatterometer images, information at local scale can be obtained. This procedure may help in extrapolating local scale phenomena to regional and global scale by considering their spatial variability.

This procedure will be further tested on other data sets and verified by also taking into account other inversion procedures.

References and Notes

1. Beven, K.J. *Rainfall-Runoff Modeling: The Primer*; John Wiley & Sons: Chichester, UK, 2001.
2. Moran, M.S.; Hymer, D.C.; Qi, J.; Sano, E.E. Soil moisture evaluation using multi-temporal Synthetic Aperture Radar (SAR) in semiarid rangeland. *Agr. For. Meteorol.* **2000**, *105*, 69-80.
3. Cosh, M.H.; Jackson, T.J.; Bindlish, R.; Prueger, J.H. Watershed scale temporal and spatial stability of soil moisture and its role in validating satellite estimates. *Remote Sens. Environ.* **2004**, *92*, 427-435.
4. Vachaud, G.; Passerat de Silans, A.; Balabanis, P.; Vauclin, M. Temporal stability of spatially measured soil water probability density function. *Soil Sci. Soc. Am. J.* **1985**, *49*, 822-828.
5. Grayson, R.B.; Western, A.W. Towards areal estimation of soil water content from point measurements: time and space stability of mean response. *J. Hydrol.* **1998**, *207*, 68-82.
6. Kachanosky, R.G.; de Jong, E. Scale dependence and the temporal persistence of spatial pattern of soil water storage. *Water Resour. Res.* **1988**, *24*, 85-91.
7. Gómez-Plaza, A.; Alvarez-Rogel, J.; Alabaladejo, J.; Castillo, V.M. Spatial patterns and temporal stability of soil moisture across a range of scales in a semi-arid environment. *Hydro. Process* **2000**, *14*, 1261-1277.
8. Martínez-Fernández, J.; Ceballos, A. Temporal stability of soil moisture in a large field experiment in Spain. *Soil Sci. Soc. Am. J.* **2003**, *67*, 1647-1656.
9. Wilson, D.J.; Western, A.W.; Grayson, R.B. Identifying and quantifying sources of variability in temporal and spatial soil moisture observations. *Water Resour. Res.* **2003**, *40*, W02507.
10. van Zyl, J.; Carande, R.; Lou, Y.; Miller, T.; Wheeler, K. The NASA/JPL three-frequency polarimetric AIRSAR system. *IEEE IGARSS Dig.* **1992**, *1*, 649-651.
11. Notarnicola, C.; Angiulli, M.; Posa, F. Use of radar and optical remotely sensed data for soil moisture retrieval over vegetated areas. *IEEE Trans. Geosci. Remote Sens.* **2006**, *44*, 925-935.
12. Notarnicola, C.; Posa, F. Inferring vegetation water content from C and L band images. *IEEE Trans. Geosci. Remote Sens.* **2007**, *45*, 3165-3171.
13. Chen, D.; Jackson, T.J.; Li, F.; Cosh, M.H.; Walthall, C.; Anderson, M. Estimation of vegetation water content for corn and soybeans with a normalized difference water index (NDWI) using Landsat Thematic Mapper data. In *Proceedings of IGARSS*, Toulouse, France, 2003; pp. 2853-2856.
14. Dubois, P.; van Zyl, J.J.; Engman, T. Measuring soil moisture with imaging radar. *IEEE Trans. Geosci. Remote Sens.* **1995**, *33*, 916-926.
15. Settle, J. On the use of remotely sensed data to estimate spatially averaged geophysical variables. *IEEE Trans. Geosci. Remote Sens.* **2004**, *42*, 620-631.

16. Wagner, W.; Pathe, C; Doubkova, M.; Sable, D.; Bartsch, A.; Hasenauer, S.; Bloeschl, G.; Scipal, K.; Martinez-Fernandez, J.; Loew, A. Temporal Stability of soil moisture and radar backscatter observed by the Advanced Synthetic Aperture Radar (ASAR). *Sensors* **2008**, *8*, 1174-1197.
17. Mohanty, B.P.; Skaggs, T.H. Spatial-temporal evolution and time-stable characteristics of soil moisture with remote sensing footprints with varying soil, slope, and vegetation. *Adv. Water Resour.* **2001**, *24*, 1051-1067.
18. Jacobs, J.M.; Mohanty, B.P.; Hsu, E.; Miller, D. SMEX02: field scale variability, time stability and similarity of soil moisture. *Remote Sens. Environ.* **2004**, *92*, 436-446.
19. Martinez-Fernandez, J.; Ceballos, A. Mean soil moisture estimation using temporal stability analysis. *J. Hydrol.* **2005**, *312*, 28-38.

© 2009 by the authors; licensee Molecular Diversity Preservation International, Basel, Switzerland. This article is an open-access article distributed under the terms and conditions of the Creative Commons Attribution license (<http://creativecommons.org/licenses/by/3.0/>).